catalysts

MDPI

Article

Photocatalytic Antibacterial Effectiveness of Cu-Doped TiO_2 Thin Film Prepared via the Peroxo Sol-Gel Method

Benjawan Moongraksathum [1], Jun-Ya Shang [1] and Yu-Wen Chen [1,2,*]

[1] Department of Chemical and Materials Engineering, National Central University, Jhong-Li 32001, Taiwan; bmoongraksathum@gmail.com (B.M.); alice19940430@gmail.com (J.-Y.S.)

[2] Department of Chemistry, Tomsk State University, 36 Lenin Prospekt, Tomsk 634050, Russia

* Correspondence: ywchen@cc.ncu.edu.tw; Tel.: +886-3422-7151 (ext. 34203)

Received: 23 July 2018; Accepted: 20 August 2018; Published: 27 August 2018

Abstract: Cu-doped titanium dioxide thin films (Cu/TiO_2) were prepared on glass substrate via peroxo sol-gel method and dip-coating process with no subsequent calcination process for the degradation of organic dye and use as an antibacterial agent. The as-prepared materials were characterised using transmission electron microscopy (TEM), X-ray diffraction (XRD), scanning electron microscopy (SEM) and X-ray photoelectron spectroscopy (XPS). For photocatalytic degradation of methylene blue in water, the samples were subjected to Ultraviolet C (UVC) and visible light irradiation. Degraded methylene blue concentration was measured using UV-Vis spectrophotometer. The antibacterial activities of the samples were tested against the gram-negative bacteria Escherichia coli (ATCC25922). Copper species were present in the form of CuO on the surface of modified TiO_2 particles, which was confirmed using TEM and XPS. The optimal observed Cu/TiO_2 weight ratio of 0.5 represents the highest photocatalytic activities under both UVC and visible light irradiation. Moreover, the same composition remarkably exhibited high antibacterial effectiveness against *E. coli* after illumination with ultraviolet A. The presence of CuO on TiO_2 significantly enhanced photocatalytic activities. Therefore, active Cu-doped TiO_2 can be used as a multipurpose coating material.

Keywords: antibacterial; copper oxide; photocatalyst; titanium dioxide; thin film; visible light

1. Introduction

Photocatalysis has garnered plenty of attention from the scientific community in recent decades, resulting in various commercialized products having photocatalytic functions. Among photocatalysts, titanium dioxide (TiO_2) has received the greatest interest because of its remarkable stability and non-toxicity. Modification of TiO_2 has been extensively studied to improve its physical and chemical properties and to overcome the limitation of TiO_2 in photocatalytic processes. Modified TiO_2 has been deployed both environmentally and hygienically, including in the photocatalytic decomposition of organic pollutants [1–5], in self-cleaning materials [6–9], and as an antibacterial agent of photo-induced photocatalytic reactions [10–13].

The activity of TiO_2 nanoparticles is due to the oxidative stress and/or the production of reactive oxygen species (ROS), including hydroxyl radical ($OH^{\bullet}$) and hydrogen peroxide (H_2O_2) under UV light irradiation; therefore, TiO_2 is used as an antimicrobial agent. The produced ROS can cause cell membrane damage, cell cycle cessation, DNA damage and lipid peroxidation in microorganisms via direct contact between cells and nanoparticles, thereby resulting in cell death [14–16].

Several transition metals are toxic to various microbial pathogens. In addition to considerable commercialization in this field, this finding has led to widespread research on the use of such materials

as practical antimicrobial agents. Among several transition metals, copper has gained considerable attention, both as dispersions and, in the case of elemental copper and as alloys [10,17,18]. For use as antibacterial agents, copper and its compounds achieve antibacterial activity by the accumulation of copper ions within cells, eventually causing degradation of cell membranes [19–21].

Using titanium tetrachloride ($TiCl_4$) as a precursor and H_2O_2 as a peptizing agent, previous studies have proposed a peroxo sol-gel method for the synthesis of neutral TiO_2 sol [22–25]. The advantages of this method include not needing a calcination process to obtain the anatase structure of TiO_2, as well as the ability to use H_2O_2 as an oxidizing agent. It results in the formation of TiO_2 nanoparticles dispersed in neutral, stable, and transparent sol.

The purpose of this study was to prepare Cu-doped TiO_2 thin films using the peroxo sol-gel method, thus determining how the addition of Cu to TiO_2 influenced its antibacterial effectiveness, as well as the photocatalytic degradation of methylene blue (MB) aqueous solution under either UVC or visible light irradiation.

2. Results and Discussion

2.1. Characteristic of Cu-Doped TiO_2 Particles

The peroxo sol-gel method was used to prepare Cu-doped TiO_2 sol by direct addition of the precursor of copper ($Cu(NO_3)_2 \cdot 3H_2O$) during the heating of TiO_2 sol. To obtain powder nanoparticles, the as-prepared sols were further dried at 70 °C for several days. The X-ray diffraction (XRD) patterns of samples are shown in Figure 1. The diffraction peaks of the TiO_2 and a series of Cu-modified TiO_2 were located at the same positions and showed a similar pattern. The diffraction peaks located at 2θ = 25.31°, 37.80°, 48.05°, 53.89°, 55.06°, 62.69°, 68.76°, and 75.03° corresponded to the anatase phase of (101), (004), (200), (105), (211), (204), (116), and (215), respectively (JCPDS 21-1272). Furthermore, no additional peaks of copper oxide or other forms were found, implying that copper oxides were either highly dispersed with little TiO_2 particles or the amount of Cu dopant was below the detection level of the technique. The size of the crystallite was calculated by the Scherrer equation [26,27]:

$$L = \frac{0.9\lambda}{\beta \cos\theta} \quad (1)$$

where λ is the X-ray wavelength (0.1540 nm), β is the full width at half maximum (FWHM), θ is the diffraction angle, and L is the average crystallite size. The results are listed in Table 1. The presence of copper slightly decreased the crystallite size of TiO_2, which was attributed to the inhibition of titania condensation and the crystallization in the Cu-doped system [21].

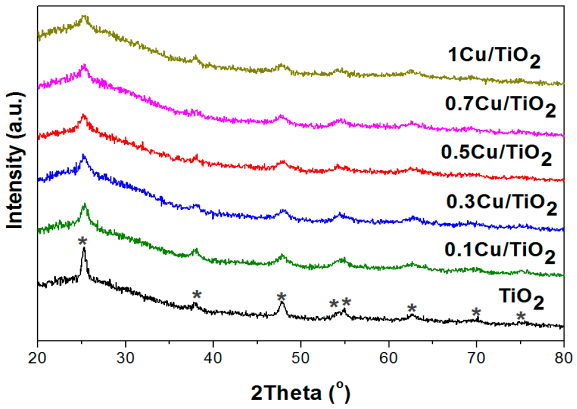

Figure 1. X-ray diffraction patterns of TiO_2 and a series of Cu-doped TiO_2 powder (* = anatase).

Table 1. Crystallite sizes of TiO_2 and a series of Cu-doped TiO_2.

Sample	Weight Ratio of Cu:TiO_2	Crystallite Size (nm)
TiO_2	0:100	14.96
$0.1Cu/TiO_2$	0.1:100	9.12
$0.3Cu/TiO_2$	0.3:100	9.40
$0.5Cu/TiO_2$	0.5:100	9.21
$0.7Cu/TiO_2$	0.7:100	9.60
$1Cu/TiO_2$	1:100	10.16

Morphology of the as-prepared samples was investigated using TEM and HRTEM. Figure 2 depicts TEM images of TiO_2 and $0.5Cu/TiO_2$ particles. The morphology of the TiO_2 particles prepared via the peroxo sol-gel method is best described as an elliptical shape with particle size of 40–60 nm and 15–30 nm for long and short axes, respectively [3,7,12,23–25]. In Figure 2b, HRTEM image displayed the lattice fringe of TiO_2 of 0.327 nm, corresponding to the anatase (101) plane. Figure 2c shows $0.5Cu/TiO_2$ particles having the particle size ranging from 20 to 30 nm and 5 to 10 nm for long and short axes, respectively. In addition, magnified view clearly identified some small copper nanoparticles ($\leq$4nm) deposited on the surface of the TiO_2 nanoparticles (see Figure 2c). Therefore, elliptical anatase TiO_2 nanoparticles can be synthesised via the peroxo sol-gel method without a subsequent annealing process, and the presence of copper could decrease the particles size and crystallite size of TiO_2, attributed to phase deterioration of the TiO_2 anatase [21].

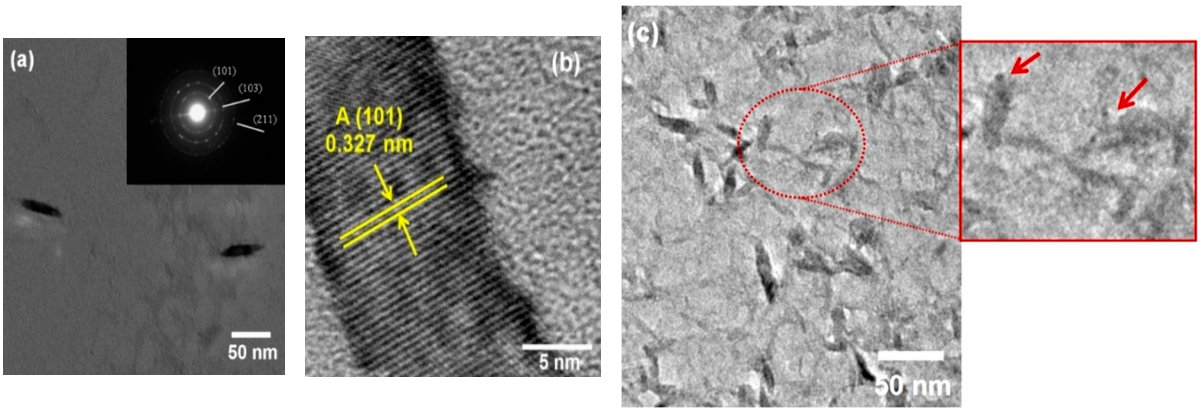

Figure 2. TiO_2 particle: (**a**) TEM image and (**b**) HRTEM micrograph representing lattice fringe attributed to the (101) plane of titania; (**c**) TEM image and magnified view of $0.5Cu/TiO_2$ particle.

2.2. Characterization of Cu-Doped TiO_2 Thin Film

XPS was performed to investigate the electronic state of each element in TiO_2 and Cu-doped TiO_2 thin films. Figure 3a–c shows the XPS spectra of Ti 2p, O 1s and Cu 2p in the TiO_2 and $0.5Cu/TiO_2$ thin films. The peaks of Ti $2p_{1/2}$ and Ti $2p_{3/2}$ in pure TiO_2 were located at 464.6 and 458.9 eV, respectively, corresponding to the tetravalent state (Ti^{4+}) [28]. The characteristic peaks of Ti 2p did not change in the presence of copper, indicating that the cations in the Cu-doped TiO_2 film are all in the Ti^{4+} state. Figure 3b shows the XPS spectra of the O 1s region for TiO_2 and $0.5Cu/TiO_2$ films. The binding state of O 1s region of TiO_2 was deconvoluted into two peaks centred at 530.7 eV and 531.7 eV, which were ascribed to lattice oxide ions in TiO_2 and hydroxyl groups on the surface, respectively (see Figure 3b and Table 2) [22]. The characteristic Cu $2p_{3/2}$ and Cu $2p_{1/2}$ peaks were observed at 934.9 eV and 954.9 eV, respectively, which were consistent with those of the Cu^{2+} cations [29]. The presence of Cu ions could capture the photogenerated carriers to accelerate the separation of charge carriers,

subsequently transferring them to the surface of TiO_2 thin film, resulting in the improvement in the photocatalytic activity of the Cu-doped TiO_2 [30].

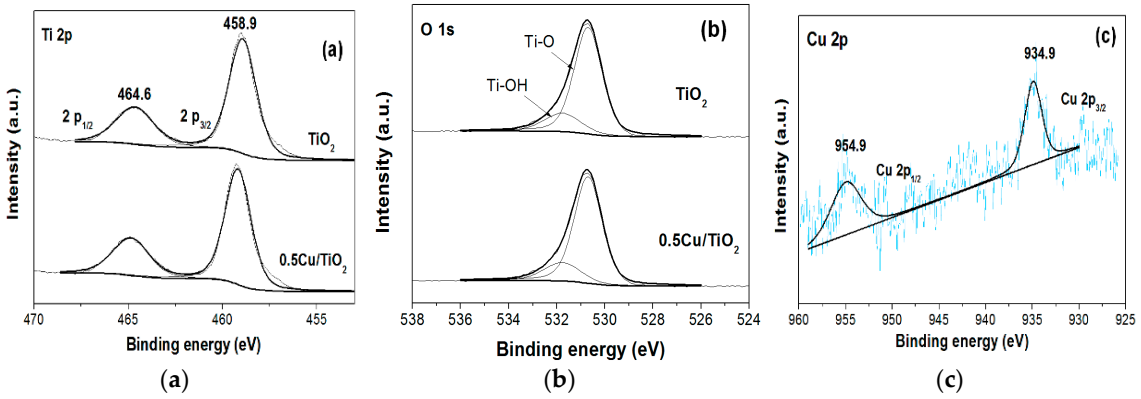

Figure 3. X-ray photoelectron spectroscopy (XPS) spectra of (**a**) Ti 2p, (**b**) O1s of TiO_2 and $0.5Cu/TiO_2$, and (**c**) Cu 2p of $0.5Cu/TiO_2$.

Table 2. O1s XPS data and the fraction of total area of TiO_2 and $0.5Cu/TiO_2$ thin films.

Sample	Lattice O^{2-}		Ti-OH	
	BE (eV)	Fraction (%)	BE (eV)	Fraction (%)
TiO_2	530.7	81.48	531.7	18.52
$0.5Cu/TiO_2$	530.6	73.72	531.6	26.28

Wettability measurements were performed using a customized in-house contact angle meter. To measure the water contact angle (WCA), a 5 µL DI water drop was dripped on the films. The TiO_2 film prepared via the peroxo sol-gel method showed hydrophilicity with an average WCA of 6.4°. After doping with copper, the average WCA of the TiO_2 dramatically increased from 6.4° to 35.9° (see Figure 4). In general, elemental copper exhibits super hydrophilicity, whereas copper oxide (e.g., CuO and Cu_2O) shows hydrophobicity. This finding confirms the presence of CuO (Cu^{2+}) in the Cu-doped TiO_2 films, which was in accordance with the XPS [31,32].

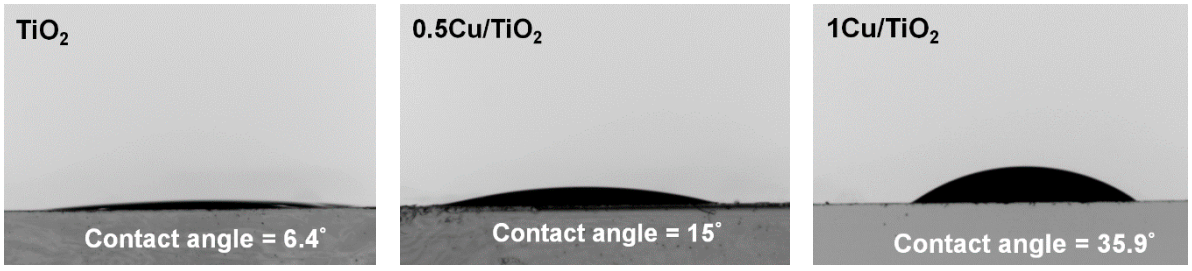

Figure 4. Water contact angle of TiO_2 and Cu-doped TiO_2 films.

2.3. Photocatalytic Degradation of MB Aqueous Solution

Prior to the photocatalytic activity, all samples were immersed into the set-up reactor and kept in the dark for 1 h to attain equilibrium adsorption of MB. The photocatalytic degradation of MB in water under UVC and visible light irradiation is shown in Figure 5. The highest photocatalytic activity under both UVC and visible irradiation was shown for the modified TiO_2 with the weight ratio $Cu:TiO_2$ = 0.5:100 ($0.5Cu/TiO_2$). The amount of copper beyond a certain loading decrease the photocatalytic activity of TiO_2 due to the Cu light absorption [33]. Furthermore, larger doping of copper resulted in CuO acting as a recombination centre [34].

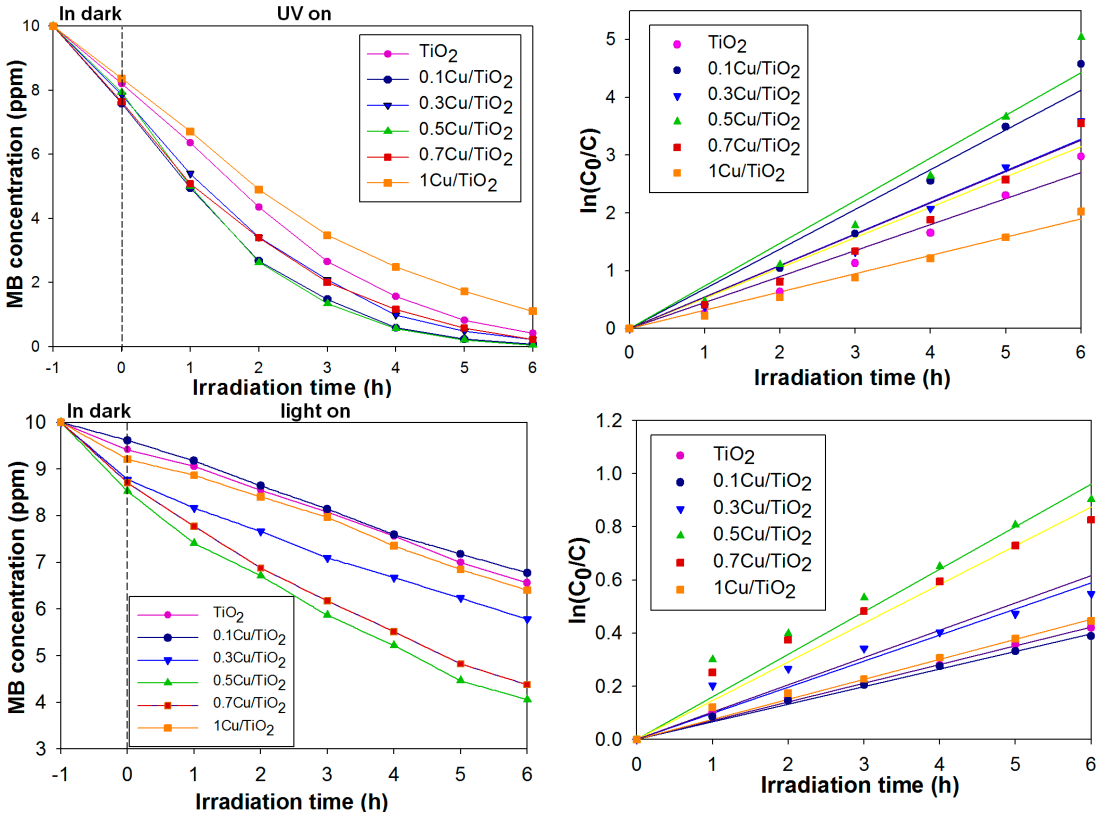

Figure 5. Photocatalytic activities of TiO_2 and Cu–doped TiO_2 films under UV light illumination (**top**) and visible light illumination (**bottom**).

The photodegradation of MB was fitted to the Langmuir–Hinshelwood model. The slope of ln (C_0/C) plotted versus irradiation time (h) indicates the reaction rate constant of the sample. Under UVC and visible light irradiation, the photocatalytic activity was the highest for $0.5Cu/TiO_2$, with a rate constant of 0.737 h^{-1} and 0.160 h^{-1}, respectively (Table 3). Higher photocatalytic activity was attributed to the photoelectron transfer of the conduction band (CB) of TiO_2 to CuO, leaving the hole on TiO_2 to take part in oxidation reaction. In other words, under UV irradiation, the presence of CuO can slow down the recombination of electron/hole pairs in TiO_2, as shown in the following equations [34,35].

$$Cu^{2+} + e^{-}CB \rightarrow Cu^{+} \quad (2)$$

$$Cu^{+} + (O_2,\ H_2O_2 \text{ or other ROS}) \rightarrow Cu^{2+} + e^{-} \quad (3)$$

CuO nanoparticles deposited on the TiO_2 surface received the photogenerated electrons from the CB of TiO_2 to form Cu^+ ion as shown in Equation (2), and Cu^+ ions could be re-oxidised to Cu^{2+} by the ROS species present in the surrounding media (3).

Table 3. Rate constant of the reaction from pseudo-first order kinetics under visible light irradiation.

Samples	Rate Constant (k, h^{-1})	
	Under UV light	Under Visible Light
TiO_2	0.449	0.070
$0.1Cu/TiO_2$	0.687	0.066
$0.3Cu/TiO_2$	0.546	0.098
$0.5Cu/TiO_2$	0.737	0.160
$0.7Cu/TiO_2$	0.524	0.146
$1Cu/TiO_2$	0.317	0.076

2.4. Photocatalytic Antibacterial Effectiveness of Cu-doped TiO_2 Thin Film

Under irradiation with UVA light, the antibacterial activity of the samples was tested against *Escherichia coli* (ATCC25922). *E. coli* is present as a normal intestinal flora and is commonly found in contaminated drinking water. After a UVA radiation of 3 h at a low UVA intensity of 33 μW/cm^2, the 0.5Cu/TiO_2 coating showed high antibacterial effectiveness of >99% when tested against *E. coli*. In contrast, TiO_2 displayed an average effectiveness of 61.20% when tested against *E. coli* (see Figure 6). Antibacterial activities of Cu-doped TiO_2 could be attributed to the production of ROS species (e.g., O_2^-, $OH^•$, and H_2O_2) using TiO_2, as well as CuO nanoparticles that trigger oxidative stress and cell damage in bacteria [36]. In addition, released Cu ions (Cu^{2+}) increased intracellular ROS in bacteria using the following pathway [17,21]:

$$Cu^+ + H_2O_2 \rightarrow Cu^{2+} + OH^- + OH\bullet \quad (4)$$

H_2O_2 is a byproduct of normal metabolism of oxygen in bacterial cells. The accumulation of ROS dramatically increased, eventually causing cell death [10,17–21,36]. Therefore, Cu-doped TiO_2 showed antibacterial effectiveness, even though a low-intensity of UVA light source was applied.

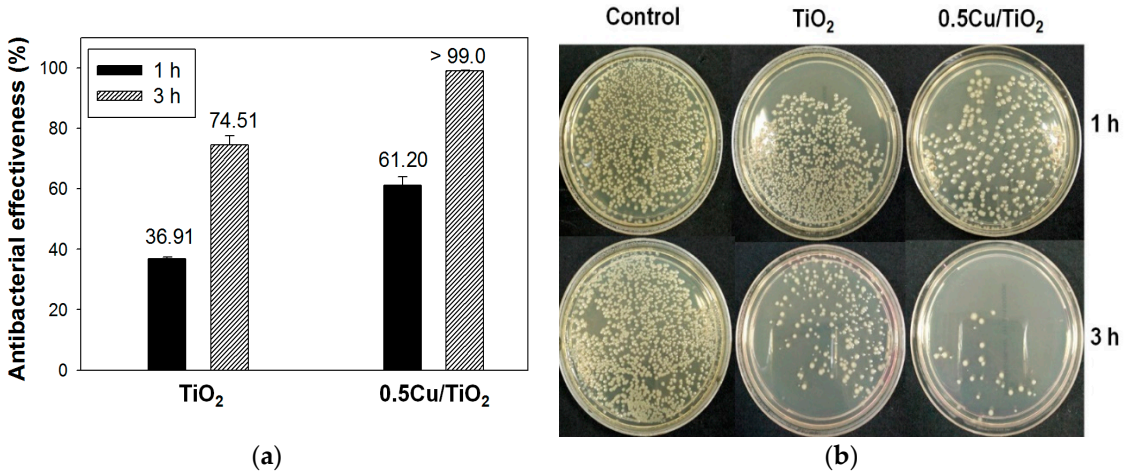

Figure 6. Antibacterial effectiveness (%) against *E. coli* following periods of illumination with 33 μW/cm^2, UVA radiation of 1 and 3 h (**a**), and counts of viable *E. coli* after incubation (1:10^3 dilution) (**b**).

3. Materials and Methods

3.1. Materials

$TiCl_4$ (purity > 99.9%) and H_2O_2 (30% in water) were purchased from Showa Chemicals Industry, Ltd. (Tokyo, Japan). NH_4OH was purchased from Merck Co. (Kenilworth, NJ, USA). Copper (II) nitrate trihydrate ($Cu(NO_3)_2 \cdot 3H_2O$) was purchased from Sigma-Aldrich (St. Louis., MO, USA). Distilled water was used throughout the experiments.

3.2. Preparation of TiO_2 and Cu-Doped TiO_2 Sol

The typical procedure of preparing TiO_2 and Cu/TiO_2 sols went as follows: Three milliliters of $TiCl_4$ were added dropwise into 150 mL 1 M HCl aqueous solution (under magnetic stirring) and kept in an ice bath so as to maintain the temperature at 0 °C for 30 min. An aqueous solution of 1 M NH_4OH was then added dropwise to form the white hydrated titanium oxide gel $Ti(OH)_4$. The pH of the solution was adjusted to 8.0 by adding the required amount of ammonia solution. After aging and stirring for 30 min, a $Ti(OH)_4$ cake was filtered and washed with distilled water until no chloride ions were detected (QUANTOFIX®). An amount of the as-prepared gel was re-dispersed in distilled water

under magnetic stirring to form a milky solution. An aqueous solution of H_2O_2 was added dropwise to the solution under vigorous stirring for 1 h. The resultant solution was heated at 95 °C for 4 h under magnetic stirring.

For preparation of Cu-doped TiO_2 sol, the copper precursor was added into the TiO_2 sol during heating at 95 °C. The solid content of the TiO_2 in the solution was 1.0 wt %; the molar ratio of H_2O_2:TiO_2 was 4:1; and the weight ratio of Cu:TiO_2 was: 0.1:100, 0.3:100, 0.5:100, 0.7:100, and 1:100. These ratios were denoted as 0.1Cu/TiO_2, 0.3Cu/TiO_2, 0.5Cu/TiO_2, 0.7Cu/TiO_2, and 1Cu/TiO_2, respectively.

3.3. Preparation of Films

The sols were aged at room temperature for 8 h before deposition on glass. The films were prepared using the dip-coating method. Soda lime glass was used as the substrate. The total coating surface area of each glass substrate was 40 cm^2. The glass substrate was cleaned using a commercial dishwashing detergent. Subsequently, it was ultrasonicated for 30 min in 1 M NH_4OH solution, thoroughly rinsed with distilled water and oven-dried at 60 °C. The glass substrate was vertically dipped into the as-prepared sol with a withdrawal speed of 30 cm/min for 7 times. The thickness of the films was 250–300 nm, as measured by SEM.

3.4. Characterization of Cu-Doped TiO_2 Particles and Thin Films

All samples were air dried at 80 °C for 1 h before further characterisation. The XRD patterns of the samples were determined using a Siemens D500 powder diffractometer (Siemens, Westborough, MA, USA) with Cu Kα source (λ = 1.5405 Å). The morphology and structure of the samples were investigated using transmission electron microscopy (TEM) on a JEM-2000 EX II (JEOL, Tokyo, Japan) operated at an accelerating voltage of 120 kV and high resolution TEM (HRTEM) on a JEOL JEM-2010 (JEOL, Tokyo, Japan) operated at 200 kV. The lattice spacing of the samples was measured using Gatan Digital Micrograph software. The chemical composition and chemical state of the samples were determined using X-Ray photoelectron spectroscopy (XPS) with a Thermo VG Scientific Sigma Prob spectrometer (Thermo Fisher Scientific, Logan, UT, USA). The XPS spectra were collected using Al K_α radiation at a voltage of 20 kV and current of 30 mA. The binding energy (BE) was calibrated using contaminant carbon (C_{1S} = 284.6 eV). The peaks of each spectrum were organised using XPSPEAK software (Thermo Fisher Scientific, Logan, UT, USA); Shirley type background and 30:70 Lorentzian/Gaussian peak shape were adopted during the deconvolution. The thickness of the films was measured using scanning electron microscopy (SEM) (Hitachi-3000, Tokyo, Japan).

3.5. Photocatalytic Degradation of MB Aqueous Solution

The photocatalytic activity of the samples was determined by inducing the decomposition of MB under irradiation with either UVC or visible light. An aqueous solution of MB (40 mL) with a concentration of 10 mg/L was loaded onto a quartz glass plate. The samples were horizontally immersed into the MB solution. Before the photocatalytic activity was measured, the reactor was kept in the dark under magnetic stirring for 1 h to achieve the saturation adsorption of MB on the coatings. The catalysts were irradiated by either two 9 W UVC lamps (wavelength = 254 nm, TUV PL-L 18W/4P 1CT/25, Philips) or two 18 W compact fluorescent lamps (1200 lumen, Philips (Pro UV Lamps Ltd., Bucks, UK)) equipped with UV cut-off filters with a cut-off wavelength of 410 nm. The distance from the lamp to the surface of the solution was 15 cm, and the concentration of the aqueous solution of MB was determined at intervals of 1 h using UV-vis spectrophotometer (JASCO V-630 (Japan Spectroscopic Company, Tsukuba, Japan)). The wavelength selected for the measurements was 663 nm, which is the characteristic maximum absorption wavelength of MB.

3.6. Study of Antibacterial Activity

The test method of the coatings against *E. coli*'s (ATCC25922) antibacterial activity was modified from the certificate "JIS Z 2801: 2000 (E)—Antimicrobial products-Test for antimicrobial activity

and efficacy" and "TN-050—Standard on nano anti-bacterial coating." The strains were grown on tryptic soy agar and diluted to 5.5×10^6–6.0×10^6 cells/mL using distilled water. The bacterial concentrations were measured from the optical density reading at 600 nm (OD_{600}). The as-prepared sols were deposited on a 5 cm × 5 cm glass substrate using the dip-coating technique and a catalyst content of 0.2 mg/cm^2. Bare glass substrates were used as controls. Before testing, all samples were sterilized and activated using two 9 W UVC light (λ = 254 nm, TUV PL-L 18W/4P 1CT/25, Philips (Pro UV Lamps Ltd., Bucks, UK)) for 1 h. In order to quantitatively evaluate the antibacterial activity of the coatings, 0.4 mL of bacterial suspension was added onto each coating. Next, the test pieces were covered with 4 × 4 cm of adhesive film (with a transparency of >85% at 340–380 nm). Covered with the adhesive film, the test piece was placed into a Petri dish and exposed to two UVA lamps (λ = 365 nm, PL-L 36W/09/4P, Philips (Pro UV Lamps Ltd., Bucks, UK)) for either 1 h or 3 h. The irradiance of the UVA intensity was measured at 33 μW/cm^2, using a UV light meter (model UV-340A, Lutron (Lutron Electronic Enterprise Co., Taipei, Taiwan)). After UVA irradiation, the bacterial suspension on each coating was washed off and diluted with phosphate buffer saline (PBS). Bacterial colony-forming units (CFUs) were enumerated by plating serial dilutions (1:10–1:10^5). The number of surviving bacterial colonies was counted (CFU/mL) after incubation at 37 °C for 24 h. The experiments were repeated three times for each sample type; therefore, three parallel CFU values were obtained for each type of sample.

The antibacterial effectiveness was calculated according to the following equation [12,25]:

$$C(\%) = \left(\frac{A - B}{A}\right) \times 100\% \quad (5)$$

where C represents antibacterial effectiveness, A is the average number of colonies formed in the blank control group (CFU/mL), and B is the average number of colonies formed in the experimental group (CFU/mL).

4. Conclusions

0.5Cu-doped TiO_2 nanoparticles can be successfully prepared via the peroxo sol-gel method without needing further calcination. The CuO nanoparticles, having a particle size of <4 nm, were deposited on the TiO_2 surface. The photocatalytic activity was the highest for 0.5Cu/TiO_2, with a rate constant of 0.737 h^{-1} and 0.160 h^{-1} under UVC and visible light irradiation, respectively. Moreover, the 0.5Cu/TiO_2 coating showed high antibacterial effectiveness of >99% against *E. coli* after illumination with 33 μW/cm^2 UVA radiation for 3 h. Therefore, the presence of CuO significantly enhanced the photocatalytic activity as well as antibacterial effect of TiO_2. Therefore, the Cu-coped TiO_2 materials prepared via the peroxo sol-gel method can be an alternative and promising solution to increasing environmental contamination.

Author Contributions: B.M. and Y.-W.C. designed the experiments; B.M. and J.-Y.S. performed the experiments, analyzed the data and contributed material characterization and analysis; B.M. wrote the paper and Y.-W.C. supervised the project.

Funding: This research was funded by MOST 107-0205-2511.

Acknowledgments: This research was supported by the Ministry of Science and Technology, Taiwan.

Conflicts of Interest: The authors declare no conflicts of interest.

References

1. Vinodgopal, K.; Wynkoop, D.; Kamat, P. Environmental photochemistry on semiconductor surfaces: Photosensitized degradation of a textile azo dye, acid orange 7, on TiO_2 particles using visible light. *Environ. Sci. Technol.* **1996**, *30*, 1660–1666. [CrossRef]

2. Mohamed, M.; Al-Esaimi, M. Characterization, adsorption and photocatalytic activity of vanadium-doped TiO_2 and sulfated TiO_2 (rutile) catalysts: Degradation of methylene blue dye. *J. Mol. Catal. A Chem.* **2006**, *255*, 53–61. [CrossRef]
3. Moongraksathum, B.; Chen, Y.W. CeO_2–TiO_2 mixed oxide thin films with enhanced photocatalytic degradation of organic pollutants. *J. Sol-Gel Sci. Technol.* **2017**, *82*, 772–782. [CrossRef]
4. Chong, M.; Jin, B.; Chow, C.; Saint, C. Recent developments in photocatalytic water treatment technology: A. review. *Water Res.* **2010**, *44*, 2997–3027. [CrossRef] [PubMed]
5. Fujishima, A.; Zhang, X.; Tryk, D. TiO_2 photocatalysis and related surface phenomena. *Surf. Sci. Rep.* **2008**, *63*, 515–582. [CrossRef]
6. Guan, K. Relationship between photocatalytic activity, hydrophilicity and self-cleaning effect of TiO_2/SiO_2 films. *Surf. Coat. Technol.* **2005**, *191*, 155–160. [CrossRef]
7. Moongraksathum, B.; Chen, Y.W. Preparation and characterization of SiO_2–TiO_2 neutral sol by peroxo sol-gel method and its application on photocatalytic degradation. *J. Sol-Gel Sci. Technol.* **2016**, *77*, 288–297. [CrossRef]
8. Sakai, N.; Fujishima, A.; Watanabe, T.; Hashimoto, K. Quantitative evaluation of the photoinduced hydrophilic conversion properties of TiO_2 thin film surfaces by the reciprocal of contact angle. *J. Phys. Chem. B* **2003**, *107*, 1028–1035. [CrossRef]
9. Watanabe, T.; Fukayama, S.; Miyauchi, M.; Fujishima, A.; Hashimoto, K. Photocatalytic activity and photo-induced wettability conversion of TiO_2 thin film prepared by sol-gel process on a soda-lime glass. *J. Sol-Gel Sci. Technol.* **2000**, *19*, 71–76. [CrossRef]
10. Sunada, K.; Watanabe, T.; Hashimoto, K. Bactericidal activity of copper-deposited TiO_2 thin film under weak UV light illumination. *Environ. Sci. Technol.* **2003**, *37*, 4785–4789. [CrossRef] [PubMed]
11. Pelaez, M.; Nolan, N.; Pillai, S.; Seery, M.; Falaras, P.; Kontos, A.; Dunlop, P.; Hamilton, J.; Byrne, J.; O'Shea, K.; et al. A review on the visible light active titanium dioxide photocatalysts for environmental applications. *Appl. Catal. B* **2012**, *125*, 331–349. [CrossRef]
12. Moongraksathum, B.; Chen, Y.W. Anatase TiO_2 co-doped with silver and ceria for antibacterial application. *Catal. Today* **2018**, *310*, 68–74. [CrossRef]
13. Verdier, T.; Coutand, M.; Bertron, A.; Roques, C. Antibacterial activity of TiO_2 photocatalyst alone or in coatings on *E. coli*: The influence of methodological aspects. *Coatings* **2014**, *4*, 670–686. [CrossRef]
14. Maness, P.; Smolinski, S.; Blake, D.M.; Huang, Z.; Wolfrum, E.J.; Jacoby, W.A. Bactericidal activity of photocatalytic TiO_2 reaction: Toward an understanding of its killing mechanism. *Appl. Environ. Microb.* **1999**, *65*, 4094–4098.
15. Castro, C.; Sanjines, R.; Pulgarin, C.; Osorio, P.; Giraldo, S.A.; Kiwi, J. Structure-reactivity relations of the Cu-cotton sputtered layers during *E. coli* inactivation in the dark and under light. *J. Photochem. Photobiol. A* **2010**, *216*, 295–302. [CrossRef]
16. Richardson, S.D.; Thruston, A.D.; Collette, T.W.; Ireland, J.C. Identification of TiO_2/UV disinfection byproducts in drinking water. *Environ. Sci. Technol.* **1996**, *30*, 3327–3334. [CrossRef]
17. Leyland, N.; Podporska-Carroll, J.; Browne, J.; Hinder, S.; Quilty, B.; Pillai, S. Highly Efficient F, Cu doped TiO_2 anti-bacterial visible light active photocatalytic coatings to combat hospital-acquired infections. *Sci. Rep.* **2016**, *6*, 24770. [CrossRef] [PubMed]
18. Litter, M. Heterogeneous photocatalysis Transition metal ions in photocatalytic systems. *Appl. Catal. B Environ.* **1999**, *23*, 89–114. [CrossRef]
19. Espirito Santo, C.; Quaranta, D.; Grass, G. Antimicrobial metallic copper surfaces kill Staphylococcus haemolyticus via membrane damage. *MicrobiologyOpen* **2012**, *1*, 46–52. [CrossRef] [PubMed]
20. Grass, G.; Rensing, C.; Solioz, M. Metallic copper as an antimicrobial surface. *Appl. Environ. Microbiol.* **2011**, *77*, 1541–1546. [CrossRef] [PubMed]
21. Rtimi, S.; Pulgarin, C.; Kiwi, J. Recent developments in accelerated antibacterial inactivation on 2D Cu-Titania surfaces under indoor visible light. *Coatings* **2017**, *7*, 20. [CrossRef]
22. Sasirekha, N.; Rajesh, B.; Chen, Y.W. Synthesis of TiO_2 sol in a neutral solution using $TiCl_4$ as a precursor and H_2O_2 as an oxidizing agent. *Thin Solid Films* **2009**, *518*, 43–48. [CrossRef]
23. Chen, Y.W.; Chang, J.Y.; Moongraksathum, B. Preparation of vanadium–doped titanium dioxide neutral sol and its photocatalytic applications under UV light irradiation. *J. Taiwan Inst. Chem. Eng.* **2015**, *52*, 140–146. [CrossRef]

24. Moongraksathum, B.; Hsu, P.T.; Chen, Y.W. Photocatalytic activity of ascorbic acid-modified TiO_2 sol prepared by the peroxo sol-gel method. *J. Sol-Gel Sci. Technol.* **2016**, *78*, 647–659. [CrossRef]
25. Moongraksathum, B.; Chien, M.Y.; Chen, Y.W. Antiviral and antibacterial effects of silver-doped TiO_2 prepared by the peroxo sol–gel method. *J. Nanosci. Nanotechnol.*. Accepted.
26. Monshi, A.; Foroughi, M.R.; Monshi, M.R. Modified Scherrer equation to estimate more accurately nano-crystallite size using XRD. *World J. Nano Sci. Eng.* **2012**, *2*, 154–160. [CrossRef]
27. Alexander, L.; Klug, H.P. Determination of crystallite size with the X–ray spectrometer. *J. Appl. Phys.* **1950**, *21*, 137–142. [CrossRef]
28. Dake, L.S.; Lad, R.J. Electronic and chemical interactions at aluminum/TiO_2 (110) interfaces. *Surf. Sci.* **1993**, *289*, 297–306. [CrossRef]
29. Su, J.; Li, Z.; Zhang, Y.; Wei, Y.; Wang, X. N-Doped and Cu-doped TiO_2-B nanowires with enhanced photoelectrochemical activity. *RSC Adv.* **2016**, *6*, 16177–16182. [CrossRef]
30. Wang, S.; Meng, K.; Zhao, L.; Jiang, Q.; Lian, J. Superhydrophilic Cu-doped TiO_2 thin film for solar-driven photocatalysis. *Ceram. Int.* **2014**, *40*, 5107–5110. [CrossRef]
31. Eshaghi, A.; Eshaghi, A. Preparation and hydrophilicity of TiO_2 sol–gel derived nanocomposite films modified with copper loaded TiO_2 nanoparticles. *Mater. Res. Bull.* **2011**, *46*, 2342–2345. [CrossRef]
32. Xu, Y.; Li, J.A.; Yao, L.F.; Li, L.H.; Yang, P.; Huang, N. Preparation and characterization of Cu-doped TiO_2 thin films and effects on platelets adhesion. *Surf. Coat. Technol.* **2015**, *261*, 436–441. [CrossRef]
33. Behnajady, M.; Shokri, M.; Taba, H.; Modirshahla, N. Photocatalytic activity of Cu doped TiO_2 nanoparticles and comparison of two main doping procedures. *Micro Nano Lett.* **2013**, *8*, 345–348. [CrossRef]
34. Moniz, S.J.A.; Tang, J. Charge transfer and photocatalytic activity in CuO/TiO_2 nanoparticle heterojunctions synthesised through a rapid, one-pot, microwave solvothermal route. *ChemCatChem* **2015**, *7*, 1659–1667. [CrossRef]
35. Janczarek, M.; Kowalska, E. On the origin of enhanced photocatalytic activity of copper-modified titania in the oxidative reaction systems. *Catalysts* **2017**, *7*, 317. [CrossRef]
36. Applerot, G.; Lellouche, J.; Lipovsky, A.; Nitzan, Y.; Lubart, R.; Gedanken, A.; Banin, E. Understanding the antibacterial mechanism of CuO nanoparticles: Revealing the route of induced oxidative stress. *Small* **2012**, *8*, 3326–3337. [CrossRef] [PubMed]